RSC Advances

ROYAL SOCIETY OF CHEMISTRY

www.rsc.org/advances

A table of contents entry

The model of core-shell MIPs was constructed to evaluate the correlation between shell thickness and binding capacity.

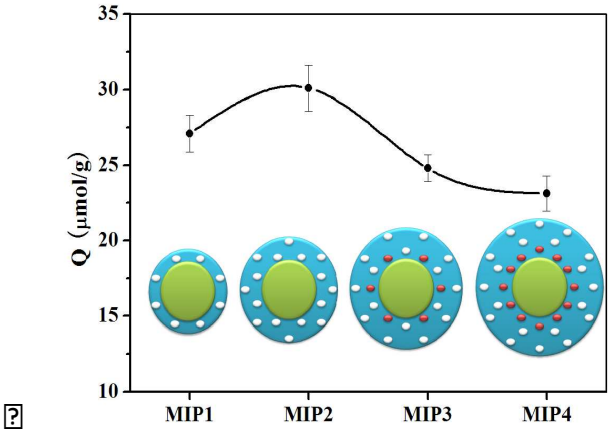

Cite this: DOI: 10.1039/c0xx00000x

www.rsc.org/xxxxxx

ARTICLE TYPE

Uniform Core-Shell Molecularly Imprinted Polymers: A Correlation Study between Shell Thickness and Binding Capacity

Zhong Zhang,[a,b] Lingxin Chen,*[a] Fangfang Yang,[a] Jinhua Li*[a]

Received (in XXX, XXX) Xth XXXXXXXXX 20XX, Accepted Xth XXXXXXXXX 20XX

DOI: 10.1039/b000000x

Core-shell molecularly imprinted polymers (CS-MIPs) have aroused increasing interests owing to its easy accessibility and favorable mass transfer. Herein, we purpose to explore the correlation between shell thickness and binding capacity by using Sudan I as template molecule to prepare different CS-MIPs at the surface of carboxyl polystyrene through emulsion polymerization with a twostep temperature-rising process. Elaborate characterizations were performed by using SEM/TEM, FT-IR, BET, TGA and so on. Main factors were systematically studied such as the amount of prepolymer solution, the amount of SDS, and the temperature step. Consequently, under the optimized conditions, the CS-MIPs with 2.60 μm of shell thickness presented the highest binding capacity of 30.1 μmol/g and the most rapid mass transfer rate. A uniform sphere model can be constructed, and template molecules located in the spherical MIPs with a diameter size of 5.20 μm will be completely effectively eluted and thereby the maximum binding capacity will be attained. The static adsorption isotherm followed the Langmuir-Freundlich adsorption model, and the fast kinetics obeyed the pseudo-second-order kinetics model. Recognition specificity for Sudan I with respect to its analogues was well displayed, with a high imprinting factor of 2.7. The establishment of critical value of shell thickness provides new insights into the preparation methodology and molecular recognition mechanism of core-shell imprinted polymers.

1. Introduction

Molecular imprinting has been widely recognized as a promising technology for the preparation of tailor-made synthetic materials that are capable of specifically recognizing targeted molecules.[1] For the past few decades, the interest and attention shown toward this technology has been increasing at an amazing pace.[1–4] This is mainly attributed to the potential diverse applications of the versatile molecularly imprinted polymers (MIPs) in purification/separation,[4–5] chemo/biosensing,[6] catalysis,[7,8] drug delivery[9,10] and so on. MIPs occupy many attractive characteristics, however, they still have met with some limitations, such as incomplete template removal, low binding capacity and slow mass transfer.[1,11] Considering the above problems, a variety of approaches have been developed, *e.g.*, precipitation polymerization, surface imprinting, controlled/living free radical polymerization, *etc*.[1] Surface imprinting has been accepted to be one of the most promising ways, with the imprinted sites situated at or close to the surface of MIPs, enabling easy access of the target molecules and fast mass transfer.[12] Surface imprinting has been extensively studied over many support materials such as silica nanoparticles,[13] silica gel, Fe_3O_4 magnetic particles,[14] and polystyrene beads[15] by many ways for the formation of surface coatings. Recently, such surface imprinting core-shell MIPs (CS-MIPs) have been increasingly synthesized and widely applied, due to its intrinsic advantages, such as good dispersion, rapid binding kinetics, easy and complete removal of template molecules.[13–17]

In order to satisfy different applications, CS-MIPs with well controlled physical forms in different size ranges are highly desirable. For examples, MIP nanoparticles are very suitable to binding assays and microfluidic separations, whereas MIP beads with diameter of 1.5–3 μm can be more appropriate to use in new analytical liquid chromatography systems. Ye and his coworkers have systematically investigated how to control particle size suitable for different analytical applications, and they synthesized monodisperse MIP beads by precipitation polymerization with different sizes in the 100 nm to 2.4 μm range by varying the ratio of two different cross-linkers.[18] Lu's group has used modified precipitation polymerization method to synthesize microspheres with diameter of about 2–3 μm.[19] The mechanism and influence factors of this polymerization method were studied. However, the researches on shell thickness for binding capacity are quite limited.[20] For instance, Zhang's group has developed a surface functional monomer-directing strategy at the surface of silica nanoparticles.[20] A critical value of shell thickness for the maximum rebinding capacity was determined by testing the evolution of rebinding capacity with shell thickness, which would provide good insights into the effectiveness of molecular imprinting and the form of imprinted materials. Therefore, by investigating the relationship of shell thickness and the imprinting performances of the CS-MIPs, it might well offer important guiding significance to attain ideal CS-MIPs.

In this work, we propose to explore the influences of shell thickness on CS-MIPs properties, by virtue of preparing Sudan I CS-MIPs at the surface of carboxyl polystyrene by core-shell emulsion polymerization with a twostep temperature-rising process. The amount of prepolymer solution, the amount of SDS, and the twostep temperature-rising polymerization were investigated and optimized to control the shell thickness of polymers. Molecular recognition properties of CS-MIPs were systematically investigated by adsorption tests, and the structural analogues were also studied for selectivity examination. Especially, the synthesis conditions and mechanism were detailed discussed, and a spherical model was constructed to evaluate the influence of shell thickness on binding capacity.

2. Experimental

2.1. Reagents

Sudan dyes (Sudan I, II, III and IV) were purchased from Shanghai Chemical Reagents Co. (Shanghai, China). Styrene, ethyleneglycol dimethacrylate (EGDMA), and methacrylic acid (MAA) were purchased from Sigma-Aldrich (Shanghai, China) and distilled under vacuum prior to use to remove inhibitor. 2,2′-Azobis(isobutyronitrile) (AIBN) was obtained from Shanghai Chemical Reagents Co. and recrystallized in methanol prior to use. Sodium dodecyl sulfate (SDS) and polyvinylpyrrolidone (PVP, MW: 24000) were supplied by Tianjin Reagent Plant (Tianjin, China). High performance liquid chromatography (HPLC) grade acetonitrile was purchased from Merck (Darmstadt, Germany). Other affiliated chemicals and reagents were all obtained from Sinopharm Chemical Reagent (Shanghai, China). All solvents and chemicals were of analytical grade and used without further purification unless otherwise specified.

2.2. Synthesis of Carboxylated Polystyrene Particles

Micrometer-sized, monodisperse carboxylated polystyrene seed particles were prepared by dispersion polymerization similar to a reported procedure with necessary modification.[21] In a brief, PVP (1.5 g) was dissolved in ethanol (95 mL) and distilled water (5 mL) in a 250 mL three-necked, round-bottom flask. The mixture was magnetically stirred under a nitrogen atmosphere. AIBN (60 mg) in styrene (10 mL) and MAA (1 mL) was added to the above solution. After poured with nitrogen for 10 min at room temperature, the polymerization reaction was heated to 60 °C for 24 h under the nitrogen atmosphere. The obtained carboxylated polystyrene particles were purified by repeated centrifugation and washing with ethanol and water (1:1, v/v) for three times, and then they were dispersed in 200 mL distilled water.

2.3. Preparation of CS-MIPs.

Sudan I CS-MIPs were prepared by core-shell emulsion polymerization based on the steps below. Prepolymer solutions were firstly prepared by dissolving Sudan I (1 mmol) and MAA (4 mmol) in toluene (4 mL), which were stored at 4 °C in refrigerator for 12 h. Then, the above prepared carboxylated polystyrene seed particles of 20 mL were added into 80 mL of aqueous solution (containing 30 mg SDS) in a 250 mL three-necked, round-bottom flask. Subsequently, 1–6 mL of the prepolymer solutions, 1–6 mL of EGDMA, and 80 mg of AIBN were added, purging with nitrogen for 10 min. The twostep temperature polymerization was undertaken with magnetic stirring in a nitrogen atmosphere at 50 °C for 2 h. The product was further aged at 60 °C for 20 h. Then the polymers were obtained by centrifugation and rinsing using anhydrous ethanol for three times to wash off residues. Afterward, the polymers were washed with methanol/acetic acid solution (9:1, v/v) in a Soxhlet extractor for 24 h to remove the template molecule. So, the Sudan I CS-MIPs were prepared. For comparison, the core-shell non-imprinted polymers (NIPs) were also prepared by using the same procedures and conditions, only without the addition of template molecule Sudan I.

In order to test the adsorption capacity of CS-MIPs, different amounts of prepolymer solutions were added for comparison. The MIPs prepared by adding different volumes of prepolymer solutions including 1, 1.5, 2, 2.5, 3 and 4 mL, were named MIP1, MIP2, MIP3, MIP4, MIP5 and MIP6, respectively, for simplicity. It should be noted that in all the preparations, the mole ratio of MAA to EGDMA was kept at a constant value of 0.2, and the amount of polystyrene seed particles was kept constant (20 mL). As a control, corresponding NIPs were prepared using identical prepolymer solutions according to the same procedures and conditions, only without the addition of template Sudan I. For example, corresponding NIP2 was given for simplicity.

2.4. Characterization.

The morphologies of polymers were observed by scanning electron microscope (SEM, Hitachi S-4800, Japan, operating at 20 kV) and transmission electron microscope (TEM, JEM-1230, operating at 100 kV). Size distribution was determined by laser particle analyzer (MASTERSIZE2000, Malvern Instruments, UK). FT-IR spectrometer (Thermo Nicolet Corporation, USA) was employed to examine the infrared spectra of samples using a pressed KBr tablet method. The thermostability and purity was tested by thermogravimetry (TG) analysis using a ZRY-2P thermal analyzer (Mettler Toledo). N_2 adsorption-desorption isotherms and structure parameters were obtained *via* Brunauer−Emmett−Teller (BET) analysis by Full-automatic Specific Surface Instruments (3H-2000BET-A, Beishide Instruments, Beijing, China). A HPLC-UV setup (Skyray Instrument Inc., China) was used for adsorption amounts evaluation.

2.5. Adsorption Experiments.

Adsorption of Sudan I from acetonitrile solutions was carried out in batch experiments. The static adsorption test was performed by allowing a constant amount of CS-MIPs to reach the adsorption equilibrium with Sudan I standard solution of known concentrations. The procedure was as follows: 20 mg of CS-MIPs were put into a 5 mL flask containing 2.0 mL of Sudan I acetonitrile solutions of various concentrations. After incubation at room temperature for 12 h, the samples was centrifuged and the supernatant solutions were collected, which was filtrated through a 0.45 μm membrane, and the concentrations of solutions were determined using HPLC-UV. The binding amount (Q) of template molecules onto MIPs could be obtained according to Equation S1, that is, by subtracting the free concentrations of template after MIPs adsorption from the initial concentrations of template molecules. The maximum binding capacity (Q_{max}) and dissociation constant (K_d) could be estimated by processing with

the following Scatchard equation:

$$\frac{Q}{C_e} = \frac{Q_{max}}{K_d} - \frac{Q}{K_d} \qquad (1)$$

where, Q is the amount of Sudan I adsorbed onto the CS-MIPs at equilibrium, C_e is the free Sudan I concentration at equilibrium, K_d is the dissociation constant, and Q_{max} is the apparent maximum amount that can be bound. K_d and Q_{max} can be obtained from the slope and intercept of the linear curve plotted in Q/C_e versus Q, respectively.

Meanwhile, the dynamic adsorption test was carried out by monitoring the temporal amount of Sudan I adsorbed by the CS-MIPs, as follows: 20 mg of CS-MIPs particles were dispersed in 2 mL acetonitrile solutions containing 3 mmol/L of Sudan I in a 5 mL flask, and then the mixture was continuously oscillated in a thermostatically controlled water bath at room temperature for 0–150 min (*i.e.*, 0, 10, 20, 30, 40, 50, 60, 90, 120 and 150 min, respectively); after that, the polymers were removed centrifugally. And the supernatant solutions were collected and determined using HPLC-UV, which was similar to that of the static adsorption test.

The same procedures were used to test the adsorption amounts of NIPs. Moreover, selectivity experiments were conducted by using Sudan II, III and IV that are structurally similar to Sudan I.

For the HPLC-UV procedure, a C_{18} column (Arcus EP-C_{18}, 5 μm, 4.6 × 150 mm Column, Waters) was used as the analytical column. HPLC conditions optimized for the Sudan dyes were as follows: mobile phase, acetonitrile/water (95:5, v/v); flow rate, 1.0 mL/min; room temperature; UV detection, 478 nm for Sudan I and 520 nm for Sudan II, III and IV; injection volume, 20 μL.

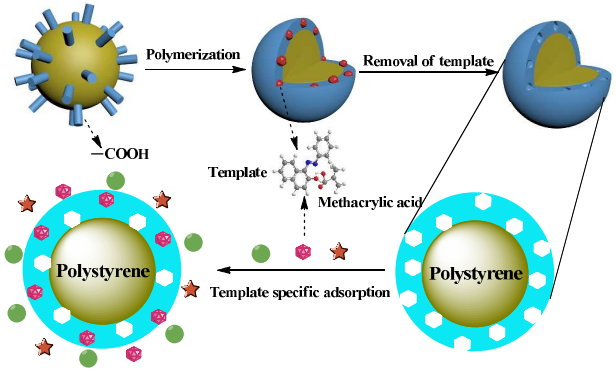

Figure 1. Schematic illustration for preparation process of CS-MIPs.

3. Results and discussion

3.1. Preparation of CS-MIPs.

Ideal imprinted materials generally require that the templates are situated at the surface or in close proximity to the materials' surface, providing the complete removal of templates, a good accessibility to the target species, and a low mass-transfer resistance. These properties are difficult to achieve in conventional bulk imprinted materials without regular shapes. In this work, emulsion polymerization was adopted. The preparation and imprinting process of the CS-MIPs is schematically illustrated in Figure 1. In the first step, carboxyl groups were introduced to the surface of polystyrene particles by dispersion

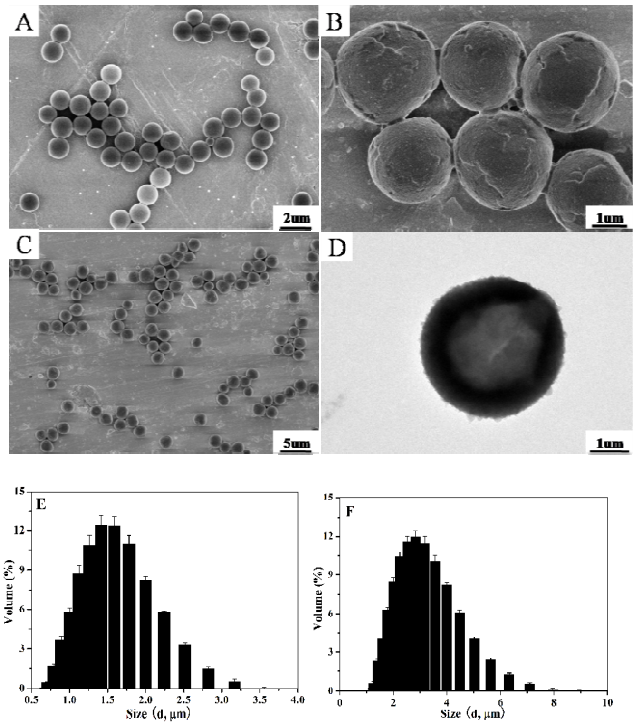

Figure 2. SEM images of (A) modified polystyrene seeds prepared by dispersion polymerization, and (B, C) CS-MIPs prepared by core-shell emulsion polymerization. (D) TEM image of CS-MIPs prepared by core-shell emulsion polymerization. Particle size distribution of (E) modified polystyrene and (F) CS-MIPs prepared by core-shell emulsion polymerization. The CS-MIPs corresponded to MIP2.

polymerization, followed by easy chemical modification using MAA for facilitating copolymerization with functional monomers. Then, the carboxyl group-capped polystyrene particles were suspended in aqueous solution with appropriate emulsifying agent (SDS). After a twostep temperature-rising emulsion polymerization, a uniform imprinting layer was coated at the surface of polystyrene particles. Finally, recognition sites located at the surface of the obtained MIPs were shaped after the removal of the template molecules. Compared to the complex surface modification for general preparation of CS-MIPs, the present procedure was simple and easy to control. Herein, three kinds of strategies were combined and successively employed to form a uniform shell. One is the twostep temperature-rising polymerization strategy. In the first polymerization stage at low temperature, polymerization proceeded slowly, resulting in that a thin oligomer layer was formed at the surface of polystyrene particles, which induced the following polymerization to occur at the surface of the polystyrene. The shell was mainly shaped during the second stage at higher temperature with faster polymerization. The following second strategy was easy to carry out by adjusting the amounts of SDS to adjust polymer's structure and size ranges. The third strategy was readily conducted by adjusting the amount of prepolymer solution to adjust shell thickness. Thus, by combining the three strategies, uniform core-shell structured MIPs could be attained.

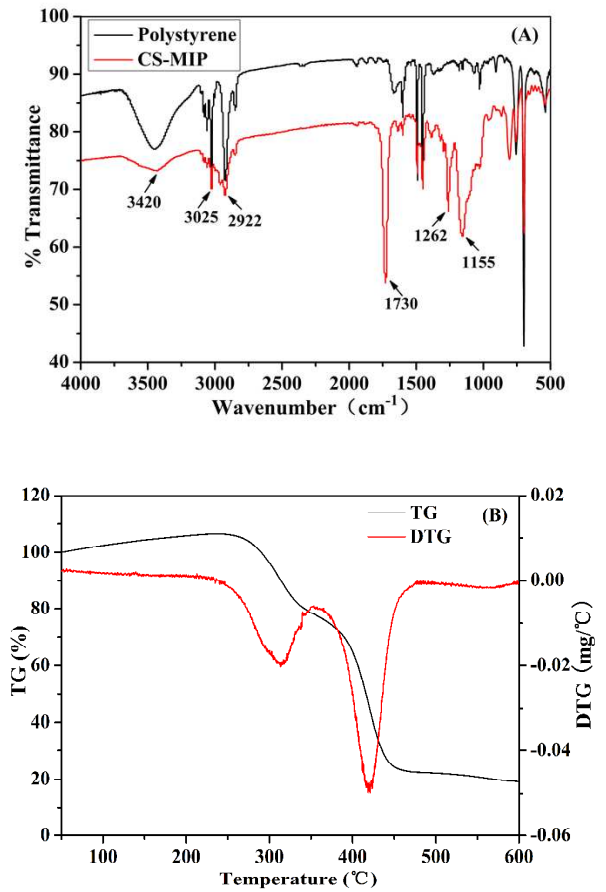

Figure 3. (A) FT-IR spectra of polystyrene and CS-MIPs (MIP2) and (B) TG/DTG curves of CS-MIPs (MIP2).

3.2.Characterization of the CS-MIPs.

The prepared CS-MIPs were elaborated characterized by SEM/TEM, laser particle analyzer, BET analysis, FT-IR and TGA. SEM and TEM were employed to capture the detailed morphologies of polystyrene and CS-MIPs. As seen in Figure 2A, the modified polystyrene particles were monodisperse with highly smooth surfaces and spherical morphology, with a uniform size of 1.5 μm. After polymerization, the MIPs possessed the rough surface with imprinted shell layer in the surface of polystyrene, and this image revealed an average diameter of about 2.9 μm (Figure 2B). Figure 2C shows the SEM image of core-shell microspheres with a relatively uniform size distribution, and the shell layer with a diameter of 700 nm could clearly be seen by TEM observation in Figure 2D. By virtue of the present three combined strategies, uniform CS-MIPs with different sizes could be synthesized. Moreover, the size distributions of microparticles were obtained by laser particle analyzer. As evidenced in Figure 2E and 2F, the intensity/volume contribution versus diameters of microparticles displayed a good size distribution and a dominant distribution peak around 1.5 μm for polystyrene and 3.0 μm for CS-MIPs, which was allowed to be overestimated comparing with that of SEM/TEM images. For unification and simplicity, the particles size data measured by laser particle analyzer were adopted for further work. In addition, by BET analysis, the specific surface area of CS-MIPs was attained of 43.27 m^2/g higher than that of corresponding NIPs (22.92 m^2/g), as seen in Table S1. Figure S1A shows N_2 adsorption-desorption isotherms of the CS-MIPs and corresponding NIPs. The average pore size of CS-MIPs and NIPs were 9.42 and 5.62 nm, respectively (Figure S1B). These results proved that the binding cavities were formed on the surface of CS-MIPs by the template molecules.

Figure 3A shows FT-IR spectra of monodisperse carboxylated polystyrene and uniform CS-MIPs. The wide and strong absorption band at around 1730 cm^{-1} could be assigned to stretching vibrations of C=O in the CS-MIPs. Two new absorption peaks at around 1262 and 1156 cm^{-1} also appeared, which could be attributed to the stretching vibration absorption of saturated C−O band in ester groups. This result indicated that ester groups in EGDMA had been successfully grafted to the surface of the polystyrene. Meanwhile, after polymerization, the wide and strong absorption band at around 3420 cm^{-1}, which could be ascribed to the stretching vibration of O−H in the carboxyl group, obviously became weak. Also, the bands at around 3025 and 2922 cm^{-1} became weak, possibly being stretching vibration of C−H in the phenyl group. So, the CS-MIPs using polystyrene as core were successfully prepared.

For TG analysis, a sample material is placed on an arm of a recording microbalance, which is placed in a furnace. The furnace temperature is controlled in a pre-programmed temperature/time profile, or in the rate-controlled mode, where the pre-programmed value of the weight change imposes the temperature change in the way necessary to achieve and maintain the desired weight-change rate. Figure 3B shows the TG and DTG curves of CS-MIPs. With the temperature increasing from 50 to 240 °C, it was strange that their weight was not decreased, which may be caused by two sides. In the first side, the rate of weight loss for CS-MIPs was very slow, and the CS-MIPs were very stable below 240 °C. In the other side, the CS-MIPs presented much higher specific surface areas. The TG analysis proceeded in the nitrogen atmosphere, and the pore structure and surface of CS-MIPs could adsorb a small amount of nitrogen. In the range of 240−350 °C, the samples loss was mainly due to the loss of polystyrene. The peak temperature of CS-MIPs was 313 °C, whereas a high rate of weight loss was presented at temperatures ranging from 350 to 470 °C, and the residue amounts were 19.38%. The weight loss was very likely to result from the decomposition of cross-linkers. Hence, the prepared CS-MIPs were fully demonstrated to occupy good thermal stability at the temperature lower than 240 °C. These observations could also be clearly explained from DTG curve.

3.3. Influence Factor Examination.

It could be clearly seen that the amounts of prepolymer solution had a significant influence on the sizes of MIPs particles, according to the preliminary experiments. The conventional mole ratio of the template molecules, functional monomers and crosslinking agents being 1:4:20 was adopted and displayed a good imprinting effect. With the fixed proportion of the three, different volumes of the prepolymer solutions were added. As shown in Table 1, with the increase of prepolymer solution, the particle size of MIPs was gradually increased. When the amounts of polymer solution increased to 4 mL, semi-solid form polymers were produced, which was a bit like that

Cite this: DOI: 10.1039/c0xx00000x

www.rsc.org/xxxxxx

ARTICLE TYPE

Table 1. Effect of Prepolymer Solution Amount on the Particle Size for Polystyrene and Polymers[a].

Polymers	Prepolymer solution (mL)	$d(0.5)$[b]	$D[3,2]$[c]	Shell thickness	Residual[d]	PDI[e]
Polystyrene	−	1.569	1.535	0	6.520%	0.227
MIP1	1	4.220	4.264	1.365	1.363%	2.75
MIP2	1.5	6.658	6.733	2.599	0.619%	0.698
MIP3	2	9.801	9.057	3.762	0.682%	3.18
MIP4	2.5	23.534	11.851	5.158	0.534%	0.639
MIP5	3	29.783	17.461	7.963	0.753%	0.601
MIP6	4	33.355	18.540	8.503	0.605%	0.7
NIP2	1.5	5.487	4.711	1.588	0.991%	2.19

(a) The data including d, D, residual and PDI were obtained from the laser particle analyzer.

(b) The diameters of 50% particles were less than the presented value in the column.

(c) The average diameter of surface area of the particle,

$$D[3,2] = \frac{\sum d^3}{\sum d^2}$$

(d) Residual will be a reliable result when the value is below 1%. The "residual" means the difference value between the experimentally determined value and predicted (fitted) value, which is directly obtained from the instrument.

(e) Polydispersity index (PDI), PDI = D_w / D_n, where, D_w and D_n mean the mass average diameter and number average diameter, respectively. Herein, PDI below 0.5 suggested a monodisperse system, ranging from 0.5 to 0.7 suggested an approximate monodisperse system, above 0.7 suggested not a monodisperse system.

prepared by bulk polymerization. So, 4 mL of prepolymer would be the boundary of emulsion polymerization and bulk polymerization. Meanwhile, the MIPs showed very poor size uniformity. When prepolymer solution was below 3 mL, particle size increased gradually with the increase of prepolymer solution; at the same time, the MIP particles were smoother and the consistency was better. When prepolymer solution was 1.5 mL, the residual and polydispersity index (PDI) were 0.619% and 0.698, respectively, which meant that the MIP particles were homogeneous. The thickness of MIP shells could further be tuned within the range of 1.3−8.5 μm by controlling the amounts of prepolymer solutions. Hence, with other reaction conditions unchanged, the shell thickness was dependent on the amount of prepolymer solution. The maximum binding capacity of six different CS-MIPs template in acetonitrile was determined. As shown in Figure S2, obviously, MIP2 prepared by using 1.5 mL prepolymer solution offered the highest binding capacity. So, 1.5 mL prepolymer solution was selected in the following experiments.

In core-shell emulsion polymerization, the amount of SDS has a significant effect on the sample particle size. Herein, the amount of SDS was investigated in order to control the polymer size. It can make mutual combination of monomer and water into a fairly stable emulsion. On the one hand, the amount of SDS cannot be too little, unless it can spread out nuclear of polystyrene stable in solution, without affecting the dispersed sample; on the other hand, if the SDS is too much, it is easy to render monomers to form small particles but not aggregate on the surface of polystyrene. As seen in Table S2, the thickness of CS-MIPs (MIP2) decreased gradually with the amount increase of SDS. The CS-MIPs using 30 mg of SDS could maintain the formation of a grafted layer in the interface of shell, showing satisfactory residual and consistency. The more SDS was, the smaller the CS-MIPs size was, but with the amount of SDS increase, CS-MIPs were also easy to form micelles, being prone to forming secondary particles of crosslinking agent. Therefore, follow-up of the related experiments were carried out by using 30 mg of SDS.

Meanwhile, in order to ensure shell layer as far as possible be fabricated on the surface of polystyrene, twostep temperature-rising polymerization was adopted with magnetically stirring in a nitrogen atmosphere at 50 °C for 2 h. The resultant product was further aged at 60 °C for 20 h.[22] At the first, the temperature was set as low as possible, the rate of polymerization reaction was set at a slow rate, to ensure that the polymerization of monomers and crosslinking agent in the solution slowly occur on the polystyrene surface to form oligomers. When the oligomers deposited on the surface of polystyrene, elevated temperature was immediately used for the rapid formation of a shell.

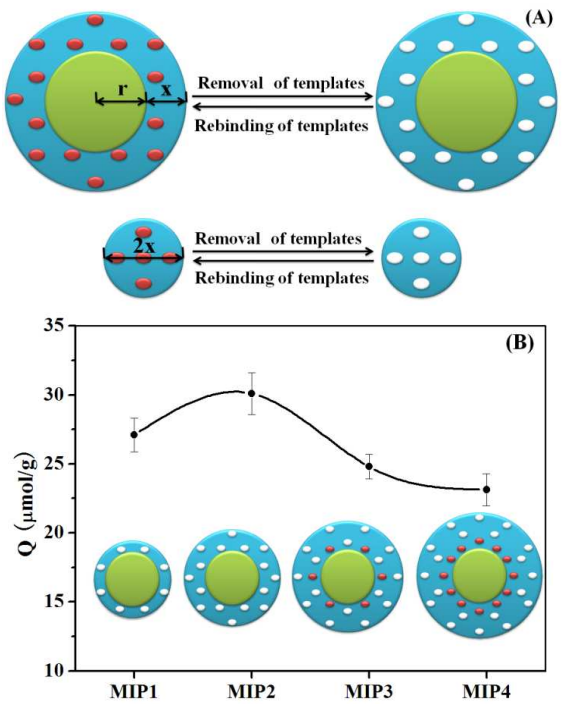

Figure 4. (A) Schematic illustration of the constructed model for the CS-MIPs. (B) Binding capacity changes of the CS-MIPs with the increase of shell thickness, and the four different MIPs have identical cores.

3.4. Model Construction.

Based on the above influence examinations, we assumed that these template molecules located within shell thickness of x from the surface could be removed by eluting solution on the core with a fixed scale of r, while when x exceeded a certain value, the template molecules in the interior imprinted sites with the highly cross-linked matrix could not be completely removed which would become invalid binding sites. The spheroidal model can be constructed as shown in Figure 4A. The effective volume of imprinted materials that can rebind target species could be defined as:

Error! Reference source not found.

$$V = \frac{4}{3}\pi[(r+x)^3 - r^3] \qquad (2)$$

In general, the r value is fixed as a certain value since the support particles were polymerized in the same way, which will not change with imprinted procedure used in the next polymerization synthesis. As seen from Figure 4B, when the x value is very small, all the imprinting molecules can be cleared off within the shell thickness of x, and the imprinting cavities can combine with template molecules rapidly. With the increase of the x value, the molecules within the particles could not be removed effectively to get effective binding sites, and thereby the binding capacity of the spherical MIP particles with identical r value in polystyrene core would be reduced (Figure 4B). As seen, the binding capacity of MIP1 was lower than MIP2, and this phenomenon might be explained that the core of MIP1 accounted for the proportion of the particles above the MIP2 and the shell of MIP1 was less than MIP2 (Table 1), however, the core of polystyrene did not have binding capacity. On the other hand, the binding capacity of MIP3 and MIP4 were lower than MIP2, because the template molecules at interior of shell became hard to elute with the increase of shell thickness, and thereby adsorption capacity also gradually reduced as well as the effective imprint sites were reduced. When forming uniform MIP particles less than a scale of $2x$, all the imprinted sites can be effectively used to binding template molecules. When the CS-MIPs possessed a diameter size of 6.73 μm (Table 1), and the solid core of polystyrene had a radius r of 0.77 μm, it was roughly concluded that all the imprinted molecules could be completely removed away from the polymers with a shell thickness x equal to or less than 2.60 μm. Thus, a uniform sphere model can be further generalized with a scale diameter of $2x$ (Figure 4A). Template molecules situated in the spherical MIPs particles with a diameter size of 5.20 μm, will be completely effectively eluted and therefore the produced cavity sites will all imprint the targeted analytes. Consequently, the maximum adsorption capacity as well the maximum imprinting efficiency will be attained.

3.5. Binding Studies of the CS-MIPs.

Figure S3A shows the binding isotherms of four different CS-MIPs and NIP2, by plotting the correlation of saturated adsorption amounts of polymers and equilibrium concentrations of Sudan I. Similar adsorption trends of the MIPs were exhibited owing to their excellent monodispersity and similar core-shell structures. MIP2 showed the highest binding capacity among the MIPs much higher than that of the corresponding NIPs (Figure S3A), and displayed the highest imprinting factor of 2.69 (Table S3), indicating MIP2 possessed excellent selectivity for template molecule. Scatchard analysis was used to assess the binding isotherms. According to the Scatchard equation, the plots for Sudan I adsorbed onto MIPs and NIPs were obtained. There were two apparent sections within the plot that can be considered as two straight lines, as shown in Figure S4, taking MIP2 as an example. The results implied that there were two types of binding sites of high and low affinity for MIPs due to imprinting,[23,24] and the rebinding/specific recognition of Sudan I was primarily dependent on hydrogen bonding. In contrast, only one straight line was observed for NIPs (data not shown), revealing that NIPs had only low affinity binding sites and were lack of imprinting process.[23,24] It also hinted that the interaction of Sudan I with NIPs was mainly from nonspecific adsorption such as van der Waals. The adsorption isotherm parameters were listed in Table S3, further confirming that MIP2 possessed the optimal molecular adsorption properties.

In addition, the ratio of the binding capacity to effective mass ratio means binding efficiency unit mass, and then the relationship between the binding efficiency unit mass and the core's radium (r) of the CS-MIPs can be provided. Consequently, according to the relationship, we can deduce the critical values which possibly results in invalid site and decreased efficiency. Take MIP2 as an example, the diameter is 6.733 μm and radius is 3.3665 μm, and then the radius of core is 0.7675 μm by subtracting the shell thickness (2.599 μm) from the radius (3.3665 μm). So, by the Equation 2, the core volume and shell volume of

the CS-MIPs could be obtained of 1.894 and 157.919 μm^3, respectively. So, the ratio of shell volume to the total volume of the CS-MIPs was 0.988, as shown in Equation S2. Owing to similar density, the shell volume ratio is just equal to mass ratio. So, the binding capacity unit mass can be attained by dividing the mass ratio by the determined binding capacity (Q), that is, 30.5 μmol/g for MIP2. The value was in good agreement with the experimentally determined value 30.1 μmol/g.

Besides, other sorption models such as Langmuir, Freundlich and Langmuir-Freundlich were also employed to further evaluate the binding isotherms, as shown in Figure S3B−D. Related model parameters were listed in Table S4. It can be observed that for all the four CS-MIPs, the Langmuir-Freundlich isotherm model yielded better fits than that by the Langmuir and Freundlich models, for correlation coefficients (R^2) above 0.99, which arises from its ability to simultaneously model both subsaturation and saturation behaviors.[25–27] Additionally, the MIP2 had the highest concentration of binding sites per gram of polymers (Nt= 126.16 μmol/g) and the largest median binding affinity (α= 0.115 g/μmol), demonstrating the excellent imprinting effect due to a number of specific binding sites on the CS-MIPs.

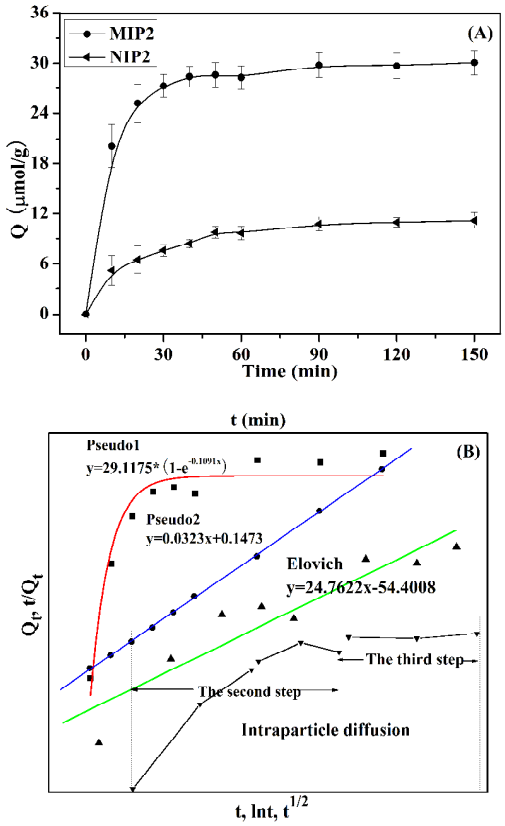

Figure 5. (A) Kinetic uptake of MIP2 and NIP2. (B) Pseudo-first-order, pseudo-second-order, Elovich and intraparticle diffusion kinetic models of MIP2. Experimental conditions: V = 2.0 mL; mass of polymer, 20 mg; adsorption time, 12 h.

Dynamic binding experiments were carried out to estimate the molecular recognition properties of the CS-MIPs by using MIP2 as an example. As can be seen from Figure 5A, a time of 40 min was needed to reach adsorption equilibrium for MIP2; in the same adsorption time, the binding capacity of MIP2 was remarkably higher than that of NIP2, indicating the uniform spherical core-shell structure of MIPs was in favor of mass transfer and binding capacity. Furthermore, the dynamic binding was investigated by using different models including pseudo-first-order, pseudo-second-order, Elovich and intra-particle diffusion,[28–30] as displayed in Figure 5B, and the obtained fitting results were summarized in Table S5. With the highest correlation coefficient of R^2=0.9997, pseudo-second-order model provided the most suitable correlation for the CS-MIPs adsorption. The pseudo-second-order equation can be expressed as:

$$\frac{t}{Q_t} = \frac{1}{k_2 Q_e^2} + \frac{t}{Q_e} \qquad (3)$$

where, Q_t is the instantaneous adsorption amount of Sudan I in the adsorbent at time t, and k_2 is the adsorption rate constant. The obtained Q_e of 31 μmol/g calculated from the pseudo-second-order model agreed well with the Q_e of 30.1 μmol/g from experimental results. The curve in the entire time period proved better for predicting the kinetic process under the same experimental conditions than other models. Therefore, it can be concluded the adsorption followed pseudo-second-order kinetics model.

The selective binding characteristic of CS-MIPs was evaluated toward competitive three Sudan dyes as structural analogues. As shown in Figure S5, the following facts can be found as follows. MIPs showed a significantly higher adsorption capacity for Sudan I than that for other competitive substrates. The adsorption capacity of NIPs for the four substrates was lower than that of MIPs. The binding capacities for Sudan II were higher than the other two as its structure is more similar to that of Sudan I. All of the above facts showed that MIPs were sensitive to the presence of Sudan I and had a good selectivity for recognition of the imprinted Sudan I molecules. The possible reason of MIPs recognizing its template molecule was due to the existence of memory cavities forming during the process of polymerization. Therefore, the molecular volume and the interaction between the target molecule and binding sites may be the two possible explanations for the selectivity of the imprinted molecule over the analogs. Obviously, the presented template played a vital role in the selectivity of molecular recognition.

4. Conclusions

In summary, new kinds of CS-MIPs microspheres were successfully prepared by core-shell emulsion polymerization in the presence of SDS *via* three combined strategies, and applied as model to explore the correlationship between shell thickness and binding capacity. The thickness of the shell is effectively controlled by optimizing the amount of prepolymer solution, the amount of SDS and twostep temperature-rising polymerization. It was deduced that all the imprinted molecules could be completely removed away from the CS-MIPs with a shell thickness equal to or less than 2.60 μm. The resultant CS-MIPs demonstrated high binding capacity and fast adsorption kinetics; the adsorption behavior was found to follow Langmuir-Freundlich isotherm and pseudo-second-order kinetic models. In addition, high selectivity was showed. A spherical model was constructed with a correlation between shell thickness and binding capacity.

Besides, the obtained CS-MIPs had an average particle size of only several micrometers, and thus they could be extended for use as highly selective packing sorbents of HPLC columns.

Furthermore, the attained correlation between shell thickness and binding capacity has important guiding significance for core-shell molecular imprinting. The combination of imprinting technology and core-shell polymers opens a new window of interest to the exploration of functionalized polymers and provides new opportunities in the applications involved in the highly selective recognition of targeted species and, therefore the high-efficiency enrichment and removal of trace analytes from complicated matrices. The studies on structural size and mechanism can not only offer an effective way to MIPs preparation, but also greatly enrich the research connotation of molecular imprinting technique.

Acknowledgements

This work was financially supported by the National Natural Science Foundation of China (21275158, 21105117), the Innovation Projects of the Chinese Academy of Sciences (KZCX2-EW-206), the 100 Talents Program of the Chinese Academy of Sciences.

[a] Key Laboratory of Coastal Environmental Processes and Ecological Remediation, Yantai Institute of Coastal Zone Research, Chinese Academy of Sciences, Yantai 264003, China
[c] University of Chinese Academy of Sciences, Beijing 100049, China
** Corresponding authors. Tel/Fax: +86 535 2109130.*
E-mail addresses: lxchen@yic.ac.cn (L. Chen); jhli@yic.ac.cn (J. Li).

Notes and references

1 L. X. Chen, S. F. Xu and J. H. Li, *Chem. Soc. Rev.*, 2011, **40**, 2922.
2 D. Cai, L. Ren, H. Z. Zhao, C. J. Xu, L. Zhang, Y. Yu, H. Z. Wang, Y. C. Lan, M. F. Roberts, J. H. Chuang, M. J. Naughton, Z. F. Ren and T. C. Chiles, *Nat. Nanotechnol.*, 2010, **5**, 597.
3 X. T. Shen, L. H. Zhu, N. Wang, L. Ye and H. Q. Tang, *Chem. Commun.,* 2012, **48**, 788.
4 Y. P. Duan, C. M. Dai, Y. L. Zhang and L. Chen, *Anal. Chim. Acta,* 2013, **758**, 93.
5 J. H. Li, Y. Y. Wen and L. X. Chen, *Chin. J. Chromatogr*., 2013, **31**, 181.
6 F. T. C. Moreira, R. A. F. Dutra, J. P. C. Noronha and M. G. F. Sales, *Biosens. Bioelectron.,* 2011, **26**, 4760.
7 G. Wulff, *Chem. Rev.,* 2002, **102**, 1.
8 J. Orozco, A. Cortés, G. Z. Cheng, S. Sattayasamitsathit, W. Gao, X. M. Feng, Y. F. Shen and J. Wang, *J. Am. Chem. Soc.,* 2013, **135**, 5336.
9 F. Puoci, G. Cirillo, M. Curcio, O. I. Parisi, F. Iemma and N. Picci, *Expert. Opin. Drug Deliv.,* 2011, **8**, 1379.
10 A. Ribeiro, F. Veiga, D. Santos, J. J. Torres-Labandeira, A. Concheiro and C. Alvarez-Lorenzo, *Biomacromolecules,* 2011, **12**, 701.
11 E. Saridakis and N. E. Chayen, *Trends Biotechnol.,* 2013, **31**, 515.
12 A. Bossi, F. Bonini, A. Turner, and S. A. Piletsky, *Biosens. Bioelectron.* 2007, **22,** 1131.
13 H. C. Chen, D. Y. Yuan, Y. Y. Li, M. J. Dong, Z. H. Chai, J. Kong and G. Q. Fu, *Anal. Chim. Acta,* 2013, **779**, 82.
14 X. P. Jia, M. L. Xu, Y. Z. Wang, D. Ran, S. Yang and M. Zhang, *Analyst,* 2013, **138**, 651.
15 L. Qin, X. W. He, W. Zhang, W. Y. Li and Y. K. Zhang, *J. Chromatogr. A,* 2009, **1216**, 807.
16 C. J. Tan, H. G. Chua, K. H. Ker and Y. W. Tong, *Anal. Chem.,* 2008, **80**, 683.
17 G. J. Guan, R. Y. Liu, Q. S. Mei and Z. P. Zhang, *Chem. Eur. J.,* 2012, **18**, 4692.
18 K. Yoshimatsu, K. Reimhult, A. Krozer, K. Mosbacha, K. Sode and L. Ye, *Anal. Chim. Acta,* 2007, **584**, 112.
19 Y. Jin, M. Jiang, Y. Shi, Y. Lin, Y. Peng, K. Dai and B. Lu, *Anal. Chim. Acta,* 2008, **612**, 105.
20 D. Gao, Z. Zhang, M. Wu, C. Xie, G. Guan and D. Wang, *J. Am. Chem. Soc.,* 2007, **129,** 7859.
21 Z. Zhang, S. F. Xu, J. H. Li, H. Xiong, H. L. Peng, L. X. Chen. *J. Agric. Food Chem.,* 2012, **60**, 180.
22 S. F. Xu, J. H. Li and L. X. Chen. *J. Mater. Chem.,* 2011, **21**, 4346.
23 H. Shaikh, N. Memon, M. I. Bhanger, S. M. Nizamani and A. Denizli. *J. Chromatogr. A*, 2014, **1337**, 179.
24 P. Luliński and D. Maciejewska, *Mater. Sci. Eng. C,* 2013, **33**, 1162.
25 R. J. Umpleby, S. C. Baxter, Y. Z. Chen, R. N. Shah and K. D. Shimizu, *Anal. Chem.,* 2001, **73**, 4584.
26 A. M. Rampey, R. J. Umpleby, G. T. Rushton, J. C. Iseman, R. N. Shah, and K. D. Shimizu, *Anal. Chem.,* 2004, **76**, 1123.
27 C. Herdes and L. Sarkisov, *Langmuir,* 2009, **25**, 5352.
28 J. M. Pan, L.Z. Li, H. Hang, R. R. Wu, X. H. Dai, W. D. Shi and Y. S. Yan, *Langmuir,* 2013, **29**, 8170.
29 J. H. Zhu, S. Y. Wei, H. B. Gu, S. B. Rapole, Q. Wang, Z. P. Luo, N. Haldolaarachchige, D. P. Young and Z. H. Guo, *Environ. Sci. Technol.,* 2012, **46**, 977.
30 S. Sadasivam, K. S. Kandasamy, P. Kalaamani, S. N.Ganapathi and T. W. Kang, *J. Chem. Eng. Data,* 2011, **56**, 4024.